Spectroscopic Properties of a Self-Assembled Zinc Porphyrin Tetramer II. Time-Resolved Fluorescence Spectroscopy

Mikalai M. Yatskou,[†] Rob B. M. Koehorst, Arie van Hoek, Harry Donker, and Tjeerd J. Schaafsma*

Laboratory of Biophysics, Department of Agrotechnology and Food Sciences, Wageningen University, Dreijenlaan 3, 6703 HA Wageningen, The Netherlands

Bas Gobets, Ivo van Stokkum, and Rienk van Grondelle

Faculty of Sciences, Division of Physics and Astronomy, Vrije Universiteit, De Boelelaan 1081, 1081 HV Amsterdam, The Netherlands

Received: January 31, 2001; In Final Form: June 17, 2001

Excited-state kinetics of complexes of a functionalized zinc tetraphenylporphyrin (ZnTPP) derivative, zinc mono(4-pyridyl)triphenylporphyrin (ZnPyP) in toluene and polystyrene/toluene mixtures have been investigated by time-resolved fluorescence spectroscopy. In addition to the ∼2.0 ns monomer fluorescence lifetime, a ≈ 1.5 ns component was found by applying global analysis to the time-resolved fluorescence decay. The 1.5 ns component is assigned to a cyclic porphyrin tetramer [Part I], with a ≈ 1 ns rotational correlation time at 10 °C. The initial fluorescence anisotropy of the monomer is found to be 0.1. In the tetramer an additional depolarization process occurs with a correlation time of ∼31 ps, resulting in a further decrease of the anisotropy from 0.1 to 0.025. This additional depolarization is ascribed to singlet energy transfer between the porphyrin units that constitute the tetramer. The intramolecular energy transfer processes have been simulated using the Monte Carlo method, yielding rate constants of $(26 \pm 4\ \text{ps})^{-1}$ and $\leq (180\ \text{ps})^{-1}$ for energy transfer between nearest neighbor and next nearest neighbor porphyrins in the tetramer.

Introduction

Energy transfer in photosynthetic light-harvesting complexes is extremely efficient even over long distances.[1,2] Although much progress has been made in describing the photophysics of such complex systems, the understanding of their excited-state dynamics is still far from complete. Many synthetic model systems have been synthesized to obtain a better insight in the energy transfer processes in natural systems.[3−12] In particular, self-assembled aggregates of metalloporphyrin arrays have been used as building blocks for artificial light harvesting systems and various molecular electronic devices.[13−16]

This work focuses on porphyrin tetramers as models for plant pigments, such as chlorophyll organized in various protein complexes because, similar to these complexes, the tetramers have a fixed, defined structure and show fast energy transfer from a particular excited porphyrin to one or more of its neighbors and loss of excitation energy by relaxation to the ground state [Part I]. Unlike photosynthetic pigment complexes, in porphyrin tetramers, these processes can be studied in isolated units in a time domain, which is experimentally much more accessible than that in the natural systems, which often exhibit extremely fast excited-state dynamics in response to optical excitation.[17−19]

This study is part of a research program aimed at understanding how the concepts of the molecular basis of photosynthesis can be used to construct artificial devices, in particular solar cells with a high photovoltaic efficiency.

From the steady-state absorption- and fluorescence spectra (Part I) it could be concluded that at low temperature, a self-assembled aggregate of ZnPyP is formed in toluene and viscous polystyrene/ toluene mixtures (PS/Tol) with a cyclic, tetrameric structure (Figure 5, Part I). This Part II reports the kinetics of the processes involving the first excited singlet state of the tetramer using time-correlated single photon counting (TCSPC) as well as streak camera detection.[20] The latter method has some distinct advantages, i.e., a time-resolution almost 10 times as high as the TCSPC method, which allows resolving fluorescence- and fluorescence anisotropy decay times of less than 1 ps. Also, the kinetics of the whole spectrum is detected instead of at a single wavelength, as with TCSPC. For streak camera measurements, the solution needs to be circulated limiting the experiments to nonviscous and noninertial solvents (e.g., toluene) and excluding viscous solvents. For this reason, all measurements on viscous PS/Tol solutions had to be done using the TCSPC method.

To understand the photophysical properties of ZnPyP tetramers, resulting from time-resolved fluorescence- and fluorescence anisotropy measurements, we also investigated unsubstituted zinc tetra(*p*-phenyl)porphyrin (ZnTPP) and its pyridine-ligated analogue as reference compounds under the same experimental conditions, but without forming aggregates. In view of its structure (Figure 1, Part I), the fluorescence lifetime of the cyclic tetramer should be close to that of pyridine ligated ZnTPP. Furthermore, note that energy transfer between the porphyrin units of the tetramer does not affect this lifetime because all monomer units of the tetramer are identical. Thus,

* To whom correspondence should be addressed. Tel: +31−317482044. Fax: + 31−317482725. E-mail: Tjeerd.Schaafsma@mac.mf.wau.nl.

[†] On leave from Department of Systems Analysis, Belarusian State University, 4, F. Scoryna Ave., Minsk, 220050, Belarus.

10.1021/jp010411h CCC: $20.00
Published on Web 11/30/2001

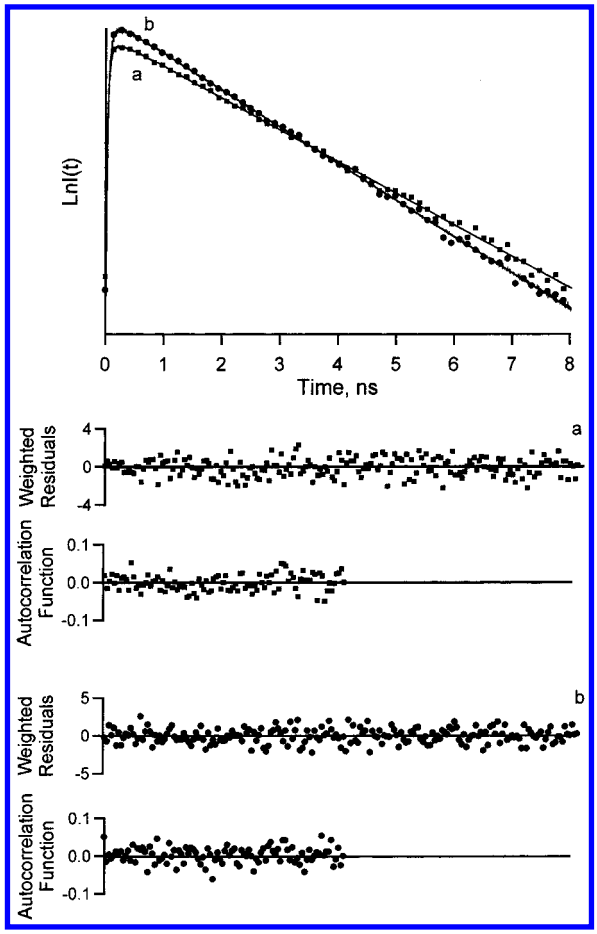

Figure 1. Experimental total fluorescence decays measured at 55 °C (a, ■) and 10 °C (b, ●), and fitted (solid lines) curves for ZnPyP; λ_{exc} = 435 nm and λ_{det} = 625 nm.

energy transfer processes within the porphyrin tetramer can conveniently be studied by investigating the fluorescence anisotropy decay.

For porphyrin monomers the time dependent fluorescence anisotropy $r(t)$ is only determined by rotational diffusion

$$r(t) = r_M^{RD}(t) \quad (1)$$

where $r_M^{RD}(t)$ is the rotational diffusion anisotropy of the monomer. On the other hand, for a porphyrin complex in solution the time dependent fluorescence anisotropy $r(t)$ can be written as a product of two independent depolarization processes

$$r(t) = r^{ET}(t) r_T^{RD}(t) \quad (2)$$

where $r^{ET}(t)$ and $r_T^{RD}(t)$ represent energy transfer within the complex and rotational diffusion of the complex itself.

The steady-state fluorescence anisotropy $r^{ET}(\infty) = \lim_{t\to\infty} r^{ET}(t) = c$ which is a time-independent constant and equals 0.025 for the tetramer in PS/Tol solution [see Part I]. The fluorescence anisotropy decay $r_T^{RD}(t)$ in eq 2 results from fully spherical rotational diffusion of the tetramer, and decays to zero in toluene solution for $t \to \infty$. Considering the size of the tetramer, for high viscosity solvents such as PS/Tol we may safely assume that the energy transfer in the tetramer is much faster than rotational diffusion. Then, for $t \to \infty$ the fluorescence anisotropy of the tetramer is given by $r(t) = cr_T^{RD}(t)$.

We applied global analysis to the TCSPC fluorescence decay components of ZnPyP in the 10 °C − 55 °C temperature range. The monomer and tetramer fluorescence lifetime components

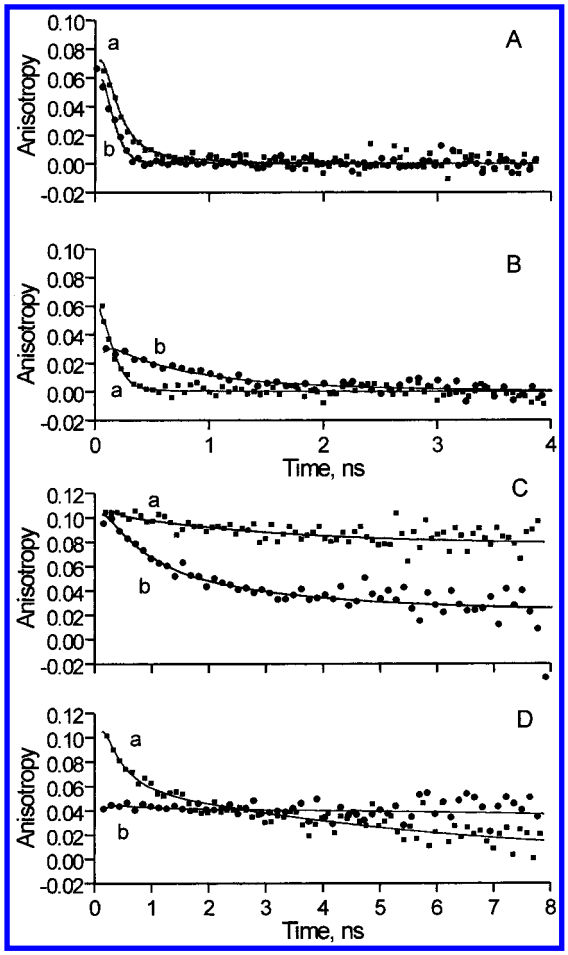

Figure 2. Experimental (■,●) and fitted (solid) curves of (A, C): ZnTPP and (B, D): ZnPyP fluorescence anisotropy in toluene (A, B) and PS/Tol (C, D) detected at 55 °C (a, ■) and 10 °C (b, ●); λ_{exc} = 435 nm; λ_{det} = 595 nm and λ_{det} = 625 nm.

were associated with their corresponding anisotropies, yielding $r_M^{RD}(t)$ and $c \bullet r_T^{RD}(t)$ of the monomers and tetramers, respectively. Global analysis has also been applied to streak camera data, yielding a time constant that describes the depolarization due to energy transfer within the tetramer. By associating the fluorescence anisotropy with the spectral properties of the tetramer, its anisotropy decay $r^{ET}(t)$ could be resolved in two time domains: one with a short decay time due to energy transfer within the tetramer and a second one with a relatively long decay time due to the rotational diffusion of the tetramer. The rate constants for singlet energy transfer within the tetramer were extracted from the fluorescence anisotropy decay $r^{ET}(t)$ using Monte Carlo simulation, yielding the rate constants for energy transfer and -relaxation processes in a rather straightforward manner.[11,21−24]

Experimental Section

Materials. ZnPyP and ZnTPP were prepared following standard procedures.[25,26] For further details, see Part I.

Time-Resolved Methods. *TCSPC Instrumentation.* The experimental setup for TCSPC has previously been described.[24,27,28] A mode-locked continuous wave Nd:YLF laser (Coherent model Antares 76-YLF, equipped with a LBO frequency doubler (Coherent model 7900 SHGTC) and BBO frequency tripler (Coherent model 7950 THG) was used to synchronously pump a continuous wave dye laser (Coherent radiation model CR 590). As a dye Coumarin 460 (Exciton Inc.)

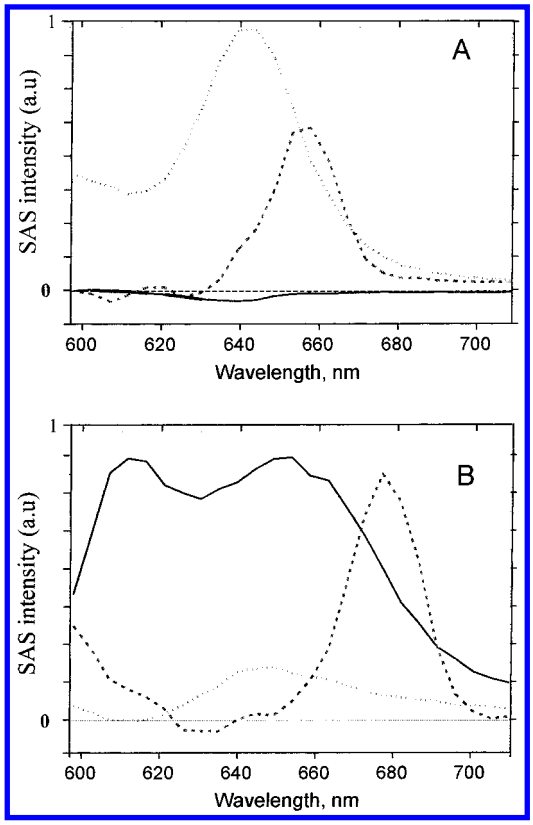

Figure 3. Species associated spectra (SAS, arbitrary units, scale 0−1) resulting from the global analysis of the polarized streak camera data sets applying an associative model (see text). (A) Temperature 55 °C, excitation wavelength 550 nm. Solid line: component of unclear origin with 83 ps isotropic lifetime; dotted line: monomers, with a 1.9 ns fluorescence lifetime and a 67 ps (amplitude 0.08) fluorescence anisotropy lifetime; dashed line: IRF-limited contribution representing Raman scattering by the solvent. (B) Temperature 10 °C, excitation wavelength 565 nm. Solid line: tetramers, with a 1.6 ns fluorescence lifetime and a 31 ps (amplitude 0.07) fluorescence anisotropy lifetime; dotted line: monomers, with a 2.1 ns fluorescence lifetime and a 0.61 ns (amplitude 0.13) fluorescence anisotropy lifetime; dashed line: IRF-limited contribution representing Raman scattering by the solvent.

was used for excitation at 465 nm. A setup with electrooptic modulators in a dual pass configuration was used to reduce the pulse rate to 594 kHz.[29] The final pulse duration of the excitation pulses was ∼4 ps fwhm and the maximum pulse energy was ∼100 pJ. To obtain a dynamic instrumental response (∼50 ps fwhm) for deconvolution purposes, the fast single-exponential fluorescence decay of Erythrosin B in water was used as a reference. The data presented were collected in a multichannel analyzer (MCA board from Nuclear Data model AccuspecB, in a PC) with a time window of 4096 channels at 2.5 ps/channel. The excitation wavelength was 435 nm and the emission wavelengths were selected by a cutoff filter (Schott KV 500) and line filters of 595 and 625 nm with a 16 nm bandwidth.

The TCSPC method has been applied to 20 μM solutions of ZnTPP in toluene, toluene/pyridine, and PS/Tol, and to 20 μM solutions ZnPyP in toluene and PS/Tol. The sample temperature was adjusted to 10, 15, 25 and 55 °C, using a cold nitrogen gas flow from an Oxford ITC4 temperature controller.

Streak Camera Detection. The experimental setup for streak camera detection has been previously described.[30] 22 μM solutions of ZnPyP in toluene were contained in a 1 cm path length glass cuvette and were thermostated either at 10 or 55 °C. The sample was refreshed using a small magnetic stirrer. The sample was excited with 100 fs pulses at 565 nm (10 °C, relatively selective for tetramers) or 550 nm (55 °C, relatively

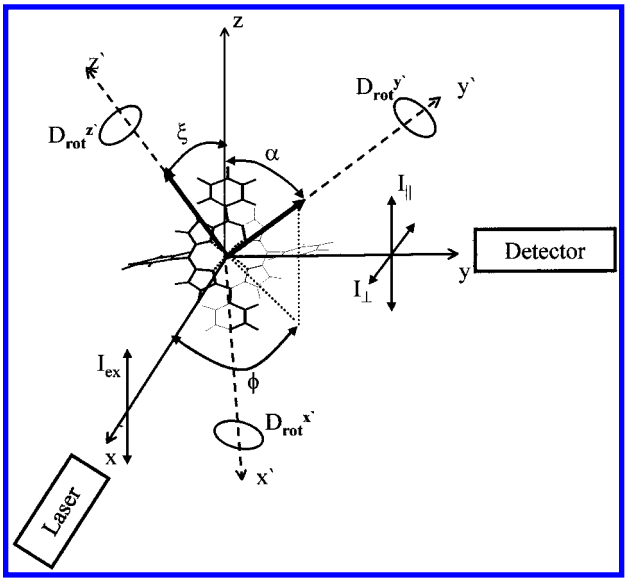

Figure 4. Schematic diagram for the measurement and simulation of parallel and perpendicular fluorescence components. The molecular coordinate system (x',y',z') has a random orientation with respect to the laboratory system (x,y,z).

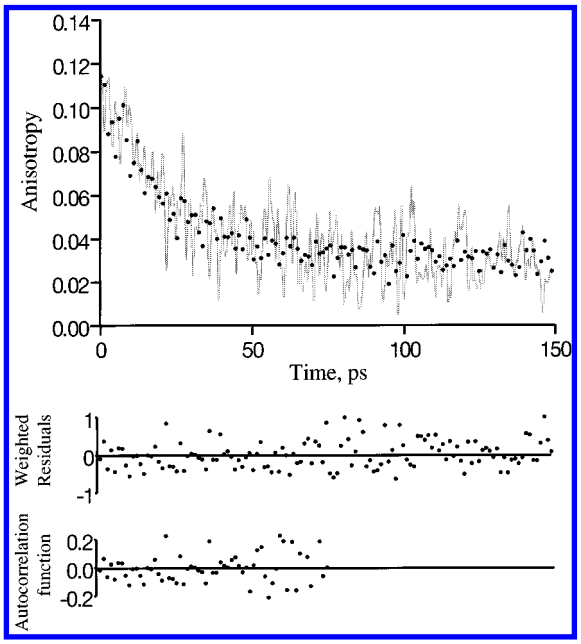

Figure 5. Examples of simulation-based fit (●) of the tetramer fluorescence anisotropy decay (−); λ_{exc}= 465 nm, λ_{det}= 612 nm; $D_{||}$ = $D_{\perp}$= 0.

selective for monomers), which were generated at a 125 kHz repetition rate using a Titanium: sapphire based oscillator (Coherent, MIRA), a regenerative amplifier (Coherent, REGA) and a double pass optical parametric amplifier (Coherent, OPA-9400). The pulse energy was typically 25 nJ. The polarization of the exciting light was alternated between horizontal and vertical. The vertically and horizontally polarized fluorescence components were detected using a Hamamatsu C5680 synchroscan streak camera equipped with a Chromex 250IS spectrograph. The instrument response function (IRF) was Gaussian shaped with a fwhm width of ∼3.5 ps. The spectral resolution was 8 nm. One streak image measured 315 nm in the spectral domain (1018 pixels) and 200 ps or 2.2 ns (1000 pixels) in the time-domain.

Time-Resolved Decay Analysis. *TCSPC*. The experimental time-resolved fluorescence decay ($I(t)$=$I_{||}(t)$ + $2I_{\perp}(t)$) was

TABLE 1: Fluorescence and Anisotropy Decay Parameters of ZnP Monomers in Toluene (Tol) and PS/Tol Solvents at Different Temperatures Using eqs 3−5

		T 55 °C				*T* 10 °C	
sample/λ_{det}	τ, ns	β_1	ϕ_1, ns	β_2	ϕ_2, ns	β_1	ϕ_1, ns
ZnP/Tol	**1.95**	0.070	**0.07**	---	---	0.073	**0.09**
597 nm	[1.94;1.97]	[0.068;0.072]	[0.06;0.09]			[0.071;0.078]	[0.08;0.11]
ZnP/Tol	**1.58**	0.068	**0.07**	---	---	0.075	**0.09**
with Pyridine	[1.55;1.62]	[0.067;0.071]	[0.06;0.08]			[0.073;0.079]	[0.08;0.10]
625 nm							
ZnP/Tol	**2.05**	0.072	**1.44**	0.022	**16.00**	0.101	**21.00**
with Pyridine	[2.04;2.07]	[0.071;0.073]	[1.38;1.52]	[0.021;0.023]	[14.00;∼]	[0.094;0.108]	[20.00;∼]
597 nm							
ZnP/PS/Tol	**1.61**	0.076	**1.62**	0.024	**17.00**	0.098	**24.00**
with Pyridine	[1.60;1.62]	[0.075;0.077]	[1.46;1.74]	[0.023;0.025]	[16.00;∼]	[0.092;0.105]	[22.00;∼]
625 nm							

The confidence intervals of the parameters, shown in square brackets, are estimated at the 95% level. The marker "∼" indicates undefined upper values of the anisotropy decay parameters. The marker "- - -" indicates the absence of a calculated parameter.

globally analyzed over a 10 °C to 55 °C temperature range and detection at 597 and 625 nm by simultaneously fitting to a sum of exponentials[31,32]

$$I(t) = \sum_{i=1}^{N} p_i \exp(-t/\tau_i) \tag{3}$$

where p_i and τ_i are the amplitude and lifetime of the *i*-th fluorescence component, respectively; *N* is the number of the fluorescence exponentials.

The parameters of the anisotropy decay $r(t) = [I_{||}(t) - I_{\perp}(t)][I_{||}(t)+2I_{\perp}(t)]^{-1}$ were retrieved using a nonassociative as well as an associative exponential model for the time-resolved fluorescence anisotropy. For the nonassociative model the fluorescence intensities $I_{||}(t)$ and $I_{\perp}(t)$ contributing to the anisotropy can be written as

$$I_{||}(t) = \sum_{i=1}^{N} A_i \exp(-t/\tau_i)[1 + 2\sum_{j=1}^{M} \beta_j \exp(-t/\phi_j)] \tag{4}$$

$$I_{\perp}(t) = \sum_{i=1}^{N} A_i \exp(-t/\tau_i)[1 - \sum_{j=1}^{M} \beta_j \exp(-t/\phi_j)] \tag{5}$$

where β_j and ϕ_j are the amplitude and the rotational correlation time of the *j*-th exponential of the fluorescence anisotropy component, and $\beta_0 = \sum_{j=1}^{M} \beta_j$ is the initial fluorescence anisotropy; *M* is the number of the anisotropy exponentials. For the associative model, $I_{||}(t)$ and $I_{\perp}(t)$ intensity components take the form

$$I_{||}(t) = \sum_{i=1}^{N} A_i \exp(-t/\tau_i)[1 + 2\sum_{j=1}^{M_i} \beta_{ij} \exp(-t/\phi_{ij})] \tag{6}$$

$$I_{\perp}(t) = \sum_{i=1}^{N} A_i \exp(-t/\tau_i)[1 - \sum_{j=1}^{M_i} \beta_{ij} \exp(-t/\phi_{ij})] \tag{7}$$

where M_i is the number of anisotropy exponentials contributed by the *i*-th fluorescence component, and ϕ_{ij} is the rotational correlation time of the *j*-th exponential of the fluorescence anisotropy contributed by the *i*-th fluorescence component. The total initial anisotropy is $\beta_0 = \sum_{i=1}^{N} \beta_{0i}$, with $\beta_{0i} = \sum_{j=1}^{M_i} \beta_{ij}$ the initial anisotropy of the *i*-th fluorescence component.

Global analysis was applied to the TCSPC data using Fluorescence Data Processor Software.[33] The accuracy of the fluorescence and anisotropy decay parameters from this analysis was estimated by the exhaustive search method.[32] The quality of the fit was judged by the χ^2 statistical criterion and by visual inspection of the time-dependent weighted residuals and their autocorrelation functions.[34]

Streak Camera. The data were globally analyzed using an associative model with two components decaying independently, each possessing its own anisotropy.[35] Thus, the data for parallel and perpendicular detection are described by

$$I_{||}(t) = \sum_{i=1}^{2} \epsilon_i(\lambda)(1 + 2\beta_{0i} \exp(-t/\phi_i))\exp(-t/\tau_i) \otimes \mathrm{IRF}(t) \tag{8}$$

$$I_{\perp}(t) = \sum_{i=1}^{2} \epsilon_i(\lambda)(1 - \beta_{0i}\exp(-t/\phi_i))\exp(-t/\tau_i) \otimes \mathrm{IRF}(t) \tag{9}$$

where ϵ_i, β_{0i}, ϕ_i, and τ_i represent the species-associated spectra, the initial anisotropy, the anisotropy decay time constant and the fluorescence lifetime of component *i*, respectively; ⊗ indicates the convolution with a Gaussian shaped instrument response function IRF(t).

Results

TCSPC Measurements. *Monomers*. For ZnTPP, a single fluorescence lifetime of 1.95 ns in toluene and 2.05 ns in PS/Tol was found. The best fit of the anisotropy decay of ZnTPP is found with a single exponential with $\phi_1 = 70$ ps/90 ps at 55 °C/10 °C for toluene as a solvent; for PS/Tol as a solvent there are two exponentials at 55 °C with $\phi_1 = 1.44$ ns, $\phi_2 = 16.00$ ns and a single exponential at 10 °C with $\phi_1 = 21.00$ ns. The initial fluorescence anisotropy of ZnTPP monomers (which do not aggregate in the temperature and concentration range of our experiments) is ∼0.07 in toluene and ∼0.1 in PS/Tol. The fits of the anisotropy decays of ZnTPP in toluene and PS/Tol at 10 and 55 °C are shown in Figure 2A and 2C. The lifetime τ, the initial anisotropies β_1 and β_2, and the rotational correlation times ϕ_1 and ϕ_2 for the ZnTPP monomers in toluene and PS/Tol are collected in Table 1.

Ligated Monomers. The same analysis of ZnTPP in the presence of excess pyridine as a ligand yielded a lifetime of 1.58 ns in toluene and 1.61 ns in PS/Tol. A fit of the anisotropy decay of ZnTPP/pyridine shows a single exponential with $\phi_1 = 70$ ps /90 ps at 55 °C/10 °C in toluene as a solvent and with two exponentials at 55 °C with $\phi_1 = 1.62$ ns, $\phi_2 = 17.00$ ns; a single exponential was found at 10 °C with $\phi_1 = 24.00$ ns in PS/Tol as a solvent. As expected, the initial anisotropy value

TABLE 2: Fluorescence- and Fluorescence Anisotropy Decay Parameters of ZnPyP in Toluene (Tol) and PS/Tol Solvents at Different Temperatures

			T 55 °C						*T* 10 °C					
sample/λ_{det}	τ_1, ns	τ_2, ns	p'_1, %	p'_2, %	β_1	ϕ_1, ns	β_2	ϕ_2, ns	p'_1, %	β_{11}	ϕ_{11}, ns	p'_2, %	β_{21}	ϕ_{21}, ns
ZnPyP in Tol	**1.97**	**1.53**	61	39	0.067	**0.08**	---	---	7	0.075	**0.10**	93	0.020	**1.00**
625 nm	[1.93;2.03]	[1.50;1.56]			[0.065;0.070]	[0.06;0.09]				[0.071;0.082]	[0.09;0.12]		[0.010;0.030]	[0.95;1.42]
ZnPyP in	**2.22**	**1.56**	48	52	0.076	**1.05**	0.025	**21.00**	16	0.100	**26.00**	84	0.025	**90.00**
PS/Tol	[2.05;2.37]	[1.48;1.61]			[0.075;0.077]	[0.97;1.48]	[0.025;0.026]	[18.00;∼]		[0.090;0.110]	[24.00;∼]		[0.023;0.025]	[80.00;∼]
625 nm														

The confidence intervals of the parameters, shown in square brackets, are estimated at the 95% level. The marker "∼" indicates undefined upper values of the anisotropy decay parameters. The marker "- - -" indicates the absence of a calculated parameter. Fluorescence decay parameters have been obtained using global analysis approach. The anisotropy decay parameters have been retrieved non-associatively (eqs 4 and 5) at 55 °C and associatively (eqs 6 and 7) at 10 °C. The relative contributions p_i', $i = 1,2$, to the total fluorescence introduced by different fluorescence components are calculated using the eq $p'_i = (p_i\tau_i)/(p_1\tau_1 + p_2\tau_2)$, $i = 1, 2$. The standard deviations of the p_i' values do not exceed 5% of their values.

of ZnTPP/pyridine is temperature-independent, and equals ∼0.07 in toluene and ∼0.1 in PS/Tol. The lifetime τ, the initial anisotropy values β_1 and β_2, and the rotational correlation times ϕ_1 and ϕ_2 for ZnTPP/pyridine in toluene and PS/Tol are collected in Table 1.

Tetramers. Assuming that the lifetime of the lowest singlet excited state of both ligated and nonligated ZnPyP is independent of temperature in the 10 °C to 55 °C range, the fluorescence decay parameters of the mixture of monomers and tetramers were determined by global analysis. Two fluorescence exponentials were found to nicely fit to all temperature-dependent ZnPyP experimental decay curves. A fit to a single exponential gave less satisfactory results and fitting with more than two exponentials did not lead to significant improvement either. The two global fluorescence components of ZnPyP in toluene have 1.97 ns and 1.53 ns lifetimes, and 2.22 ns and 1.56 ns for PS/Tol as a solvent. In toluene and PS/Tol the relative contribution of the 1.53−1.56 ns fluorescence component to the total fluorescence reaches 90% and 84% at 10 °C and 39% and 48% at 55 °C, respectively. Figure 1 shows two experimental fluorescence decays detected at 625 nm at 10 °C and 55 °C, and the result of the global analysis using two exponentials. The ZnPyP anisotropy associated with the different fluorescence components measured at 10 °C could be appropriately analyzed using single exponentials with rotational correlation times ϕ_{11} = 100 ps/26.00 ns and ϕ_{21} = 1.00/90.00 ns in toluene and PS/Tol for the 1.97−2.22 ns and 1.53−1.56 ns lifetime components, respectively. The ZnPyP anisotropy decay at 55 °C was analyzed using an associative as well as a nonassociative model, of which only the latter gave reliable results, yielding a single exponential (ϕ_1 = 80 ps) in toluene and two exponentials (ϕ_1 = 1.05 ns and ϕ_2 = 21.00 ns) in PS/Tol. The initial anisotropy value of the 1.97−2.22 ns fluorescence component is 0.076 and 0.1 in toluene and PS/Tol, respectively, whereas the initial anisotropy value of the 1.53−1.56 ns fluorescence component was considerably lower, i.e., 0.020 and 0.025 in toluene and PS/Tol, respectively. The results of the fits of the anisotropy decay of the ZnPyP in toluene and PS/Tol at 10 and 55 °C are shown in Figure 2B and 2D. The results of the fluorescence global analysis with associative as well as nonassociative anisotropy for ZnPyP in toluene and PS/Tol are presented in Table 2.

Streak Camera Measurements. Using the streak camera faster kinetics of the tetramer is accessible than with the TCSPC method, including energy transfer within the tetramer. Because the streak camera measures the time evolution of the whole fluorescence spectrum rather than at single wavelengths, the monomer and tetramer spectra associated with different fluorescence- and fluorescence anisotropy lifetimes could be resolved. These species-associated fluorescence spectra for ZnPyP in toluene at 10 °C and 55 °C are shown in Figure 3.

Monomers. Figure 3A shows the results of the measurements at 55 °C. The dominating contribution has a spectrum (dotted curve) which peaks at 642 nm. The fluorescence lifetime of this component is 1.9 ± 0.2 ns, whereas the rotational correlation time is 67 ± 7 ps. These combined data are a clear indication that this component represents the monomers. A small ∼83 ps rising component (solid curve) was also necessary to obtain a good fit of the data, the nature of which is presently unknown.

The monomer species, corresponding to the spectrum in Figure 3B, detected at 10 °C (dotted curve) with a peak around 645 nm, has a fluorescence lifetime of 2.1 ± 0.2 ns and a rotational correlation time of 0.61 ± 0.06 ns, with an amplitude of 0.13 ± 0.01. The dashed component in Figure 3A and −B, which peaks at 656 and 677 nm, respectively, represents a pulse-limited contribution, assigned to a Raman scattering line of toluene 2900 cm^{-1} red shifted with respect to the excitation wavelength.

Tetramers. Figure 3B shows the species-associated spectra for ZnPyP in toluene at 10 °C, at which temperature monomers and tetramers coexist. To record intramolecular energy transfer in the tetramers 565 nm was used for excitation, which is relatively selective for this species. The solid line in Figure 3B represents a spectrum with maxima around 612 and 652 nm of a species with a 1.6 ± 0.2 ns fluorescence lifetime and a ∼31 ps rotational correlation time with a 0.07 ± 0.01 relative amplitude. The fluorescence spectrum and lifetime of this species were basically identical to those found in the TCSPC measurements, indicating that this species is the tetramer. We therefore conclude that the 31 ps anisotropy decay reflects energy transfer within the tetramer. The relative amplitude of this decay component agrees with the expected initial anisotropy of 0.1. The small contribution with ∼0.02 relative amplitude of the anisotropy decay in the nanosecond region due to rotational diffusion, that was observed in the TCSPC measurements, was not resolved by the streak-camera measurements.

Discussion

TCSPC Results. *ZnTPP Monomers.* The 1.95−2.05 ns lifetimes for monomeric, nonligated ZnTPP collected in Table 1 are in good agreement with literature.[36−39] The slight increase of the lifetime in PS/Tol as compared to that in toluene is considered to be a medium effect. The fluorescence anisotropy decay $r(t)$ of ZnTPP in toluene is a single exponential (Table 1), in agreement with published results.[36,40−42] However, the fluorescence anisotropy $r(t)$ of ZnTPP monomers in PS/Tol cannot be fitted to a single exponential at 55 °C. In viscous solutions the fluorescence anisotropy $r(t)$ of a planar molecule such as the ZnTPP monomer is given by[36]

$$r(t) = \beta_0\,[0.25\exp(-6D_\perp t)+0.75\exp(-(2D_{||}+4D_\perp)t)] \quad (10)$$

where $D_{||}$ and $D_\perp$ are the in-plane and out-of-plane rotational diffusion coefficients. Equation 10 is a double exponential and fits the experimental data of ZnTPP in PS/Tol at 55 °C very well. The best fitted parameters collected in Table 1 show that the preexponential factors β_1 and β_2 are close to those in eq 10. The upper limits of the 95% confidence intervals of the rotational correlation times corresponding to the largest β_2 value cannot be determined with sufficient accuracy because in viscous solution the correlation times are longer than the 8 ns experimental time window. The ZnTPP anisotropy decay measured in PS/Tol solution at 10 °C can be approximated by a single exponential. The second slower anisotropy component is not found at 10 °C presumably again due to the 8 ns experimental time window and the slowing down of the rotation at this temperature. The initial anisotropy value β_0 for the ZnTPP in PS/Tol is ~0.1 in good agreement with both the predicted values[43,44] and published data.[7,45] We found a somewhat lower value of 0.07−0.08 for β_0 for the porphyrin monomers in the nonviscous solvent toluene, resulting from the relatively fast rotational diffusion with a 80−100 ps correlation time in this solvent.

Ligated ZnTPP Monomers. Ligation of ZnTPP to pyridine results in shortening of the fluorescence lifetime to 1.58−1.61 ns in both solvents. The slight increase of the lifetime in PS/Tol as compared to that in toluene is again ascribed to a medium effect. Ligation of ZnTPP with pyridine does not significantly change the anisotropy decay parameters (Table 1), so that the previous discussion of the results for nonligated ZnTPP also applies to its ligated analogue.

ZnPyP Monomers and Tetramers. Following the previous analysis of the monomer fluorescence- and fluorescence anisotropy decay of ZnTPP monomers in toluene and PS/Tol, we now apply the same method to the porphyrin tetramer. Note that the anisotropy decays in both solvents are expected to be affected by the energy transfer processes within the tetramer, and thus by the porphyrin aggregate structure.

Using global analysis to retrieve the ZnPyP fluorescence components, we attribute the 1.97−2.22 ns lifetime to the nonligated monomers in view of the results for ZnTPP in Table 1. The 1.53−1.56 ns fluorescence lifetime is close to the 95% confidence interval of the lifetime of pyridine-ligated ZnTPP, and thus likely corresponds to the ligated ZnPyP unit in the tetramer. Similarly, the increase of the relative contribution of the 1.53−156 ns fluorescence component to 84% and 93% in toluene and PS/Tol, respectively, by lowering the temperature to 10 °C can be explained by the temperature-dependent intramolecular ligation of the porphyrin units resulting in formation of a cyclic tetramer as shown in Figure 5 (cf. Part I). At 55 °C ligated porphyrins in toluene and PS/Tol still contribute 39% and 52%, respectively, to the total fluorescence. This relatively large contribution, even at 55 °C, results from the fact that the excitation was around 435 nm, closest to the Soret band maximum of the ligated species at 430 nm, whereas the fluorescence was detected at 625 nm, again corresponding to the ligated species. The increase in the fraction of the ligated species changing the solvent from toluene to PS/Tol reflects the lower solubility of porphyrins in the latter solvent.

The ZnPyP rotational correlation time $\phi_{11} = 100$ ps in toluene at 10 °C associated with the 1.97 ns lifetime is of the same order as that of ZnTPP under the same experimental conditions and therefore is assumed to reflect the monomer anisotropy. The anisotropy associated with the 1.53 ns lifetime is also a single exponential in toluene at 10 °C but now with a long $\phi_{21} = 1.00$ ns rotational correlation time, which is characteristic for rotation of the aggregate, assuming that the energy transfer is much faster then rotational diffusion. From the associative analysis of the anisotropy decay of ZnPyP in toluene at 10 °C, we conclude that ϕ_{21}, associated with the 1.53 ns fluorescence component, is about 10 times longer than ϕ_{11} of the monomer at the same temperature (Table 1). Describing the rotational dynamics of porphyrin monomers and -tetramers in toluene by single ϕ_{11} and ϕ_{21} values and approximating the tetramer as a sphere, its effective rotational radius ρ_{Tetr} can be related to that of the monomer ρ_M as follows from the Stokes−Einstein-Debye-Perrin relation[46]

$$\rho_{Tetr} = (\phi_{11}/\phi_{21})^{-1/3}\rho_M \quad (11)$$

The radius of the solvent cavity in which the tetramer rotates is calculated to be almost twice that of the porphyrin monomer and quite close to the radius calculated from the tetramer vacuum structure using the Chem-X program.[47] Although this finding may not be considered as unambiguous evidence for a tetrameric aggregate, it certainly points to a cyclic, closed structure. The same conclusions as for ZnPyP in toluene apply to the PS/Tol solution, i.e., that (i) the anisotropy decay parameters of ZnPyP associated with the 2.22 fluorescence component closely agree with those for ZnTPP; (ii) the rotational correlation time associated with the 1.56 fluorescence component is longer than that for ZnTPP monomers; (iii) the rotational correlation time of the tetramer in PS/Tol solution is less accurate than in toluene as a result of the 8 ns experimental time window. The ZnPyP anisotropy at 55 °C analyzed with a nonassociative model reflects almost the same anisotropy parameters as for the ZnTPP monomers in both solvents (cf. Tables 1 and 2).

The initial β_{11} anisotropy value of the ZnPyP monomer in PS/Tol at 10 °C, associated with the 1.97−2.22 ns fluorescence component is ~0.075−0.100 in both solvents, in good agreement with the ZnTPP monomer values (cf Tables 1,2 and Figure 2). The β_{21} value of 0.025, associated with the 1.53−1.56 ns fluorescence component at 10 °C, is approximately four times smaller than for the porphyrin monomer in toluene and PS/Tol (cf Tables 1,2 and Figure 2). From this finding, we may conclude that fast internal energy transfer occurs between the porphyrin units within the tetramer, resulting in effective fluorescence depolarization. This is also noticeable for toluene as a solvent but less unambiguous than for PS/Tol, since rotational motion may also affect the anisotropy decay. Taking into account that energy transfer processes are at least one order faster than the 1.58 ns lifetime and its associated rotational correlation time, then the observed initial anisotropy β_{21} is expected to reflect the relative orientations of the porphyrin molecules in the aggregate. Following Figure 6 of Part I the theoretical value for β_{21} is calculated to be 0.025, in very good accordance with the experimental results (Table 2) and the steady-state anisotropy (Part I, Figure 4B).

Streak Camera Results. *ZnPyP Monomers and Tetramers.* Just as with the TCSPC method, lifetimes of 1.6 and 1.95−2.10 ns were found for the ZnPyP tetramer and the monomer by applying the global analysis to the fluorescence decays. The 67 ps rotational correlation time associated with the monomer spectrum at 55 °C agrees with that previously observed for the monomers using the TCSPC method. At 10 °C a 0.61 ns rotational correlation time is found, definitely higher than the 100 ps value from TCSPC measurement. This long anisotropy component is most likely resulting from a less accurate

resolution of the associated long rotational correlation times. Taking into account that at 10 °C the tetramer concentration is much higher than that of the monomers and noting the relation $\beta^{Mon}\phi_{rot}{}^{Mon} \approx \beta^{Tetr}\phi_{rot}{}^{Tetr}$ for the anisotropy parameters, the 0.61 ns correlation time actually constitutes the mean value of the monomer and tetramer rotational correlation times weighted with their relative contributions, basically in agreement with the results of TCSPC data analysis. The 31 ps component, that only could be observed at the higher time resolution of the streak camera, obviously must be assigned to energy transfer within the tetramer.

Following this critical evaluation of the various TCSPC- and streak camera results, now the rate constants for energy transfer processes within the tetramer can be quantitatively determined. This is done by analyzing the experimental time-resolved fluorescence anisotropy decay detected at 612 nm making use of Monte Carlo simulations and adopting a hopping model for energy transfer within the tetramer.

Monte Carlo Simulations. The Monte Carlo algorithm for generating the fluorescence- as well as the anisotropy decay closely follows previously developed procedures.[22,48] Figure 4 schematically presents the basic principles for collecting the parallel and the perpendicularly polarized components of the porphyrin monomer fluorescence. It is important to note that this monomer scheme can be extended to that for the tetramer by assuming four connected porphyrin monomers fixed in a molecular coordinate system attached to one of the monomers in the aggregate. The contributions of the tetramer to the fluorescence intensities $I_{||}$ and $I_{\perp}$ for the initially excited and next nearest porphyrin within the tetramer is given by

$$P_{I||} \sim 3/4\,(1 - \sin^2\alpha \sin^2\phi)\,(\cos\phi\cos\alpha\cos\xi - \sin\phi\sin\xi + \cos\phi\sin\alpha)^2 \quad (12)$$

$$P_{I\perp} \sim 3/4\,(1 - \sin^2\alpha \sin^2\phi)\,(-\sin\alpha\cos\xi + \cos\alpha)^2 \quad (13)$$

and for the nearest neighbors to the left and right of the initially excited porphyrin unit

$$P_{I||} \sim 3/8\,(1 - \sin^2\alpha \sin^2\phi)\,(\sqrt{3}\cos\phi\cos\alpha\cos\xi - \sqrt{3}\sin\phi\sin\xi + \cos\phi\sin\alpha)^2 \quad (14)$$

$$P_{I\perp} \sim 3/8\,(1 - \sin^2\alpha \sin^2\phi)\,(-\sqrt{3}\sin\alpha\cos\xi + \cos\alpha)^2 \quad (15)$$

where $P_{I||}$ and $\boldsymbol{P}_{I\perp}$ denote the probabilities of the $I_{||}$ and $I_{\perp}$ fluorescence components; α and ϕ are the spherical coordinates of either one of the degenerate emission moments with respect to the laboratory coordinate system; ξ is a third angle defining the orientation of the molecular coordinate system with respect to that of the laboratory. In general, the anisotropy decay is determined by the geometry of the tetramer by the rotational diffusion coefficients $D_{rot}{}^{x'}$, $D_{rot}{}^{y'}$, $D_{rot}{}^{z'}$ and the energy transfer rate constants. For the monomer porphyrin $D_{rot}{}^{x'} = D_{rot}{}^{y'} = D_{\perp}$, and $D_{rot}{}^{z'} = D_{||}$ for rotational diffusion around the x', y', z' molecular coordinate axes.

The simulation of the energy transfer processes in the tetramer is based on random hopping of the excitation energy. Starting from an initially excited molecule, the excitation visits the porphyrin monomer units in the tetramer until the event of emission. The time spent by the hopping excitation from the moment of initial excitation till emission is considered as one run in the simulation procedure. The schematic diagram of excitation hopping in the tetramer has been presented in Figure 6 of Part I. The probabilities for excitation hopping between neighboring units are denoted P_N, and between units at opposite sides of the tetramer P_A. With P_τ, the probability for fluorescence emission, P_N, P_A, P_τ are related by $P_N + P_A + P_\tau = 1$. The Monte Carlo random walk starts by generating an initial orientation of the tetramer, in particular an orientation of the initially excited molecule i with its coordinate system $(x',y',z')_i$ [48] in the laboratory coordinate system (x,y,z). Next, excitation hopping is simulated using a random numbers generator and introducing starting values for the probabilities P_N, P_A, P_τ.[22] The procedure is repeated until the event of fluorescence emission. At the last step of the simulation run the total time Δt elapsed after a number of energy transfer hops following one excitation is stored either as the "parallel" or the "perpendicular" component using eqs 12−15,[48] yielding two histograms, which are the source for the simulated anisotropy decay.

Finally, we note that the probabilities P_N, P_A, P_τ are inversely proportional to the corresponding energy transfer hopping times $\tau^{ET}{}_N$, $\tau^{ET}{}_A$, and the tetramer fluorescence lifetime τ^{tetr}, respectively. We simulated 10^7 excitation runs, which ensured a combination of an acceptable signal-to-noise ratio, stable values of χ^2, and a reasonably short simulation time. Isolated monomer porphyrins were excluded from the simulations because associative anisotropy analysis showed a negligible contribution of the monomers to the total emission under the experimental conditions (10 °C, $\lambda_{exc} = 565$ nm; $\lambda_{det} = 612$ nm). Energy transfer between the tetramers and the singlet−singlet annihilation are also not considered because of the low molar porphyrin concentration and excitation rates. Because the analysis is limited to a 200 ps time window rotational diffusion of the tetramers need not be considered since both $\tau^{ET}{}_N$ and presumably $\tau^{ET}{}_A \ll \phi_{tetr} \approx 1$ ns (Table 2).

The lifetimes $\tau^{ET}{}_N$, $\tau^{ET}{}_A$, and τ^{Tetr} were used to fit the simulated anisotropy decay to the experimental decay curve, employing a published fitting algorithm.[49,50] The 95% confidence intervals of the simulated decay parameters were estimated using the method of asymptotic standard errors.[34]

As shown in Figure 5, the experimental tetramer anisotropy decay at 612 nm could be nicely fitted with the following set of parameters: $\tau^{ET}{}_N = 26 \pm 4$ ps, $\tau^{ET}{}_A = 190$ ps, implying that the rate constant for energy transfer across the tetramer is bounded as $0 \le k^{ET}{}_A \le (180\text{ ps})^{-1}$, and $\tau^{tetr} = 1.5 \pm 0.1$ ns. Note, however, that the value of (190 ps) $^{-1}$ for the $(\tau^{ET}{}_A)^{-1}$ rate constant may have an uncertainty due to cross-correlation with the rotational correlation time ϕ_{tetr} of the tetramer. As expected, the rate constant for energy transfer between neighboring porphyrins is found to be much larger than across the tetramer, explaining the fast depolarization in the initial part of the anisotropy decay.

As an additional test of the simulations we calculate the anisotropy of a nonrotating tetramer in the 8 ns time window, implying $D_{||} = D_{\perp} = 0$. The Monte Carlo simulations of experiments under these conditions result in an initial anisotropy value of 0.025, in close agreement with the experimental initial anisotropy β_{21} (Table 1).

If all four porphyrin planes in the tetramer are indeed perpendicular, as shown in Figure 6 of Part I, then there is no overlap between the π-orbitals of any two porphyrin monomers, and consequently no energy transfer by the exchange mechanism. Then the rate constants for energy transfer coming out of the Monte Carlo simulations should agree with those calculated with a Förster type of energy transfer.[51] Using a point dipole model the energy transfer rate constant k_{ET} follows from

$$k_{ET} = \kappa^2 \tau^{-1} (R_0/R)^6 \quad (16)$$

with

$$R_0{}^6 = 9 \times 10^{-25} Q n^{-4} J \quad (17)$$

where κ is the orientation factor, τ is the lifetime of the energy donor, R_0 is the critical transfer distance (Förster radius), R is the center-to-center distance between energy donor and − acceptor, Q is the absolute excitation yield of the unquenched energy donor, n is the solvent refractive index, and J is the overlap integral of the donor fluorescence spectrum with the acceptor absorption spectrum. Using the absorption and emission spectra of ZnPyP at 10 °C, the overlap integral was calculated to be $\sim 8.5 \bullet 10^{-15}$ $M^{-1}cm^{-1}$. With $Q = 0.04$,[52] and $n_{toluene} = 1.49$[53] in eq 18 it follows that $R_0 \approx 19$ Å. The center-to-center distances R between neighbor and next nearest neighbor molecules in the tetramer were determined from a molecular model to be 10 and 14 Å. Substituting these data in eq 16 and using $\kappa_{||} = 1$ and $\kappa_{\perp} = 0.5$ for parallel (||) and perpendicular (⊥) transition dipole moments wrt the 4-fold symmetry axis z (Part I, Figure 6), the Förster rate constants k_{ET} are calculated to be $\sim(32\ ps)^{-1}$ and $\sim(190\ ps)^{-1}$ for energy transfer between molecules I−II/I−IV and I−III, respectively. Note that the $(190\ ps)^{-1}$ rate constant is the result of the sum of two rate constants $(240\ ps)^{-1}$ and $(960\ ps)^{-1}$ calculated with orientation factors $\kappa = 1$ and $\kappa = 0.5$, respectively (Part I, Figure 6) for the transition moments of molecules I and III.

The $\sim(32\ ps)^{-1}$ rate constant is close to that of the Monte Carlo simulations, whereas the $(190\ ps)^{-1}$ calculated using eq 16, equals the abovementioned simulated upper limit. The total rate constant for energy transfer from a particular excited porphyrin in the tetramer to any of the other porphyrins, is calculated to be $(23 \pm 3\ ps)^{-1}$ using the Monte Carlo simulations. This result is in fair agreement with the averaged $(31\ ps)^{-1}$ rate constant, which we already calculated by global fitting of the experimental anisotropy decays at 10 °C.

The porphyrin units in the tetramer structure of Figure 5 of Part I are in fact so close, that one may wonder whether the point dipole model, used to calculate the Förster rate constants is justified at all. We found that the use of the extended-dipole model[54] does not significantly alter the conclusions of this work and changes the abovementioned results by no more than 10%. The good agreement between the experimental and calculated Förster energy transfer rate constants nicely confirms the tetramer structure presented in Figure 5 of Part I.

Conclusions

- Lowering the temperature of solutions of ZnPyP in toluene and polymer/toluene results in formation of cyclic tetramers via zinc-pyridyl ligation as can be concluded from the ligation shifts and splitting of the Soret band in the visible absorption spectra (Part I). Consistent with this observation, the monomer fluorescence with a 1.95−2.22 ns lifetime is accompanied by a 1.53−1.56 ns lifetime component, assigned to ligated porphyrin units. The 1.5 ns fluorescence component is associated with a rotational correlation time of ∼1 ns, as compared to ∼100 ps for the monomer, in agreement with the tetramer/monomer size ratio.
- Both the steady-state anisotropy spectrum and the fluorescence anisotropy decay of ZnPyP at 10 °C are in agreement with internal energy transfer resulting in fluorescence depolarization and a static value of 0.025 for the fluorescence anisotropy. The anisotropy decay parameters are shown to be in accordance with a tetrameric structure of the aggregate.
- It follows from Monte Carlo simulations, that the rate constants for energy transfer between nearest and next nearest neighbors are $\sim(26\ ps)^{-1}$ and $\sim(190\ ps)^{-1}$, respectively. These rate constants are in agreement with a Förster energy transfer mechanism and support a tetramer structure with all four porphyrin monomers mutually perpendicular.
- This work demonstrates that Monte Carlo simulation of time-resolved fluorescence and anisotropy data is powerful tool to determine the structure and the excited state kinetics of self-assembled porphyrin aggregates in solution. Because this method is not limited to solutions, it is expected to be generally applicable to interacting dyes including solid dye films.

Acknowledgment. The authors want to thank Prof. V. V. Apanasovich, Dr. E. G. Novikov, Mr. A. Digris, Mr. V. Skakun for useful discussions and Prof. A. J. W. G. Visser for useful comments and help with the Fluorescence Data Processor Software. The research at the VU (B.G., IHMvS, RvG) was supported by The Netherlands Organization for Scientific Research (NWO) through the Foundation of Earth and Life Sciences (ALW). M.M.Y. was supported by a Wageningen University Ph.D. Fellowship (Sandwich Program).

References and Notes

(1) van Grondelle, R.; Dekker, J. P.; Gillbro, T.; Sundström, V., *Biochim. Biophys. Acta* **1994**, *1187*, 1.
(2) Sundström, V.; Pullerits, T.; van Grondelle, R. *J. Phys. Chem. B* **1999**, *103*, 2327.
(3) Prodi, A.; Indelli, M. T.; Kleverlaan, C. J.; Scandola, F.; Alessio, E.; Gianferrara, T.; Marzilli, L. G. *Chem. Eur. J.* **1999**, 5, 2668.
(4) van Patten, P. J.; Shreve, A. P.; Lindsey, J. S.; Donohoe, R. J. *J. Phys. Chem. B* **1998**, *102*, 4209.
(5) Li, F.; Gentemann, S.; Kalsbeck, W. A.; Seth, J.; Lindsey, J. S.; Holten, D.; Bocian, D. F. *J. Mater. Chem.* **1997**, *7*, 1245.
(6) Lawrence, D.; Jiang, I.; Levett, M. *Chem. Rev.* **1995**, *95*, 2229.
(7) Maiti, N. C.; Mazumdar, S.; Periasamy, N. *J. Phys. Chem. B* **1998**, *102*, 1528.
(8) Alessio, E.; Gremia, S.; Mestroni, S.; Iengo, E.; Srnova, I.; Slof, M. *Inorg. Chem.* **1999**, *38*, 869.
(9) Shachter, A. M.; Fleischer, E. B.; Haltiwanger, R. C. *J. Chem. Soc. Chem. Commun.* **1998**, 60.
(10) Leray, I.; Verniéres, M. C.; Pansu, R.; Bied-Charreton, C.; Faure, J. *Thin Solid Films* **1997**, *303*, 295.
(11) Sato, N.; Ito, S.; Sugiura, K.; Yamamoto, M. *J. Phys. Chem. A* **1999**, *103*, 3402.
(12) Kerp, H. R.; Donker, H.; Koehorst, R. B. M.; Schaafsma, T. J.; Van Faassen, E. E. *Chem. Phys. Lett.* **1998**, *298*, 302.
(13) Barbara, P. F.; Meyer, T. J.; Ratner, M. A. *J. Phys. Chem.* **1996**, *100*, 13148.
(14) Yamazaki, I.; Tamai, N.; Yamazaki, T.; Marakami, A.; Mimuro, M.; Fujita, Y. *J. Phys. Chem.* **1988**, *92*, 5035.
(15) Wasielewski, M. R. *Chem. Rew.* **1992**, *92*, 435.
(16) Wasielewski, M. R.; Gaines, G. L., III; Weiderrecht, G. P.; Svec, W. A.; Niemczyk, M. P. *J. Am. Chem. Soc.* **1993**, *115*, 10 442.
(17) Gradinaru, C. C.; Pascal, A. A.; van Mourik, F.; Robert, B.; Horton, P.; van Grondelle, R.; van Amerongen, H. *Biochemistry* **1998**, *37*, 1143.
(18) Gradinaru, C. C.; Özdemir, S.; Gülen, D.; van Stokkum, I. H. M.; van Grondelle, R.; van Amerongen, H. *Biophys. J.* **1998**, *75*, 3064.
(19) Gradinaru, C. C.; van Stokkum, I. H. M.; Pascal, A. A.; van Grondelle, R.; van Amerongen, H. *J. Phys. Chem. B* **2000**, *104*, 9330.
(20) Lakowicz, J. R., Ed., *Topics in Fluorescence Spectroscopy*, Vol. 1; Plenum Press: New York, 1991.
(21) Johansson, L. B. -Å.; Engström, S.; Lindberg, M. *J. Phys. Chem.* **1992**, *96*, 3845.
(22) Andrews, L.; Demidov, A., Eds., *Resonance Energy Transfer*; John Willey & Sons Ltd Inc: New York, 1999.
(23) Yatskou, M. M.; Donker, H.; Koehorst, R. B. M.; van Hoek, A.; Schaafsma, T. J. *Chem. Phys. Lett.*, in press.
(24) Donker, H.; Koehorst, R. B. M.; van Hoek, A.; van Schaik, W.; Yatskou, M. M.; Schaafsma, T. J. *J. Phys. Chem. B*, submitted.
(25) Adler, A. D.; Longo, F. R.; Finarelli, J. D.; Goldmacher, J.; Assour, J.; Korsakoff, L. *J. Organic Chem.* **1967**, *32*, 476.

(26) Adler, A. D.; Longo, F. R.; Kampas, F.; Kim, J. *J. Inorg. Nucl. Chem.* **1970**, *32*, 2443.
(27) Visser, A. J. W. G.; van den Berg, P. A. W.; Visser, N. V.; van Hoek, A.; van den Burg, H. A.; Parsonage, D.; Claiborne, A. *J. Phys. Chem. B* **1998**, *102*, 10 431.
(28) van den Berg, P. A. W.; van Hoek, A.; Walentas, C. D.; Perham, R. N.; Visser, A. J. W. G. *Biophys. J.* **1998**, *74*, 2046.
(29) van Hoek, A.; Visser, A. J. W. G. *Rev. Sci. Instruments* **1981**, *52*, 1199.
(30) Gobets, B.; van Stokkum, I. H. M.; Rögner, M.; Kruip, J.; Kleima, F. J.; Schlodder, E.; Karapetyan, N. V.; Dekker, J. P.; van Grondelle, R. *Biophys. J.*, submitted.
(31) Marquardt, D. W. *J. Soc. Ind. Appl. Math.* **1963**, *11*, 431.
(32) Beechem, J. M. *Methods Enzymol.* **1992**, *210*, 37.
(33) Digris, A. V.; Skakun, V. V.; Novikov, E. G.; van Hoek, A.; Claiborne, A.; Visser, A. J. W. G. *Eur. Biophys J.* **1999**, *28*, 526.
(34) Bevington, P. R. *Data Reduction and Error Analysis for the Physical Sciences*; McGraw-Hill: New York, 1969.
(35) Kleima, F. J.; Hofmann, E.; Gobets, B.; van Stokkum, I. H. M.; van Grondelle, R.; Diederichs, K.; van Amerongen, H.; *Biophys. J.* **2000**, *78*, 344.
(36) Maiti, N. C.; Mazumdar, S.; Periasamy, N. *J. Phys. Chem.* **1995**, *99*, 10708.
(37) Lindsey, J. S.; Delaney, J. K.; Mauzerall, D. C.; Linschitz, H. *J. Am. Chem. Soc.* **1988**, *110*, 3611.
(38) López-Cornejo, P.; Costa, S. M. B. *Langmuir* **1998**, *14*, 2042.
(39) Fonda, H. N.; Gilbert, J. V.; Cormier, R. A.; Sprague, J. R.; Kamioka, K.; Connoly, J. S. *J. Phys. Chem.* **1993**, *97*, 7024.
(40) Millar, D. P.; Shah, R.; Zewail, A. H. *Chem. Phys. Lett.* **1979**, *66*, 435.
(41) Dutt, G. B.; Doraiswamy, S.; Periasamy, N.; Venkataraman, B. *J. Chem. Phys.* **1990**, *93*, 8498.
(42) Roy, M.; Doraiswamy, S. *J. Chem. Phys.* **1991**, *94*, 5360.
(43) Knox, R. S.; Gülen, D. *Photochem. Photobiol.* **1993**, *57*, 40.
(44) Wynne, K.; Hochstrasser, R. M. *Chem. Phys.* **1993**, *171*, 179.
(45) Gouterman, M.; Stryer, L. *J. Phys. Chem.* **1962**, *37*, 2260.
(46) Atkins, P. W. *Physical Chemistry* Oxford University Press: Oxford, 1998.
(47) *Chem-X* Chemical Design Ltd: Oxon, England, 1993.
(48) Harvey, S. C.; Cheung, H. C. *Proc. Natl. Acad. Sci. U.S.A.* **1972**, *69*, 3670.
(49) Apanasovich, V. V.; Novikov, E. G.; Yatskou, M. M. *J. Appl. Spec.*, in press.
(50) Apanasovich, V. V.; Novikov, E. G.; Yatskov, N. N. *Proc. SPIE*, Advances in Fluorescence Sensing Technology III **1997**, *2980*, 495.
(51) Förster, T. *Ann. Physik.* **1948**, *2*, 55.
(52) Harriman, A.; Porter, G.; Searle, N. *J. Chem. Soc., Faraday Trans. 2* **1979**, *75*, 1515.
(53) *Handbook of Chemistry and Physics*; CRC Press: Cleveland, Ohio 44128, USA, 1974.
(54) Czikklely, V.; Forsterling, H. D.; Kuhn, H. *Chem. Phys. Lett.* **1970**, *6*, 207.